Rotation Radius Dependence of ^{123}I-FP-CIT and ^{123}I-IBZM SPECT Uptake Ratios: A Monte Carlo Study

Anne Larsson[1], Susanna Jakobson Mo[2], and Katrine Riklund[2]

[1]Department of Radiation Sciences, Radiation Physics, Umeå University, Umeå, Sweden; and [2]Department of Radiation Sciences, Diagnostic Radiology, Umeå University, Umeå, Sweden

In dopamine brain SPECT, semiquantitative techniques are in use, mostly for research purposes, to calculate activity uptake in the striatum relative to the background. The measured uptake ratios depend on both acquisition and reconstruction, and one important parameter is the rotation radius of the γ-camera detectors, which affects spatial resolution. In brain SPECT research studies, the rotation radius is typically set to a constant value to maintain a constant resolution, but because of variations in patient anatomy and compliance, this is not always possible. **Methods:** In this study, correction factors as a function of rotation radius are developed to correct the uptake ratios where the rotation radius has deviated from the reference value, 15 cm. Monte Carlo simulations of a digital brain phantom were used to produce images with a high and a low uptake ratio, and for both studies the rotation radius was varied between 14 and 23 cm. Two different methods, one based on 2-dimensional (2D) regions of interest of constant shape and size, and one based on predefined 3-dimensional (3D) volumes of interest, were used to calculate the semiquantitative uptake ratios. **Results:** For the 2D method, the change in uptake ratio was 1.2%/cm for the high uptake ratio and 0.9%/cm for the low uptake ratio. The corresponding results for the 3D method were 2.1% and 1.7%, respectively. **Conclusion:** The 3D method was found to be more dependent on rotation radius than the 2D method, which was expected because of the 3D nature of the partial-volume effect. The correction factors were, however, less dependent on which of the 2 uptake ratios was simulated, which is positive for the application of the correction equations on patient data.

Key Words: SPECT; rotation radius; ^{123}I; FP-CIT; IBZM

Dopamine SPECT has potential to be a valuable diagnostic tool for parkinsonian syndromes (*1*). The most commonly used radioligand for dopamine transporter SPECT, ^{123}I-FP-CIT ([123]I-*N*-ω-fluoropropyl-2β-carbomethoxy-3β-(4-iodophenyl)

nortropane, or ^{123}I-ioflupane [DaTscan; GE Healthcare B.V.]), has affinity to the presynaptic dopamine transporter protein in the striatum. This characteristic has been shown to be useful for differentiating idiopathic Parkinson disease from essential tremor (*2*), idiopathic parkinsonism, and drug-induced parkinsonism (*3–5*). Striatal uptake of ^{123}I-FP-CIT is reduced in idiopathic Parkinson disease patients, compared with healthy controls, and can be very low in advanced stages of the disease. The radiopharmacon ^{123}I-IBZM ([123]I-(*S*)-2-hydroxy-3-iodo-6-methoxy-*N*-[1-ethyl-2-pyrrodinyl)-methyl]benzamide [^{123}I-Iolopride; GE Healthcare B.V.]) is a dopamine receptor antagonist that has a high affinity to D_2- and D_3-receptors (*6,7*). ^{123}I-IBZM SPECT is claimed to have a differential diagnostic value in the issue of idiopathic Parkinson disease or atypical parkinsonism (i.e., multiple-system atrophy or progressive supranuclear palsy) (*8,9*). The activity uptake in the striatum has been shown to be decreased in patients with atypical parkinsonism but should typically be normal or increased in idiopathic Parkinson disease (*9,10*). Both ^{123}I-FP-CIT SPECT and ^{123}I-IBZM SPECT have become frequently performed examinations at the University Hospital of Umeå, because of the ongoing prospective population-based Parkinson study NYPUM (*11*). ^{123}I-FP-CIT SPECT is also a frequently performed clinical examination.

In both ^{123}I-FP-CIT and ^{123}I-IBZM brain SPECT, semiquantitative techniques applying regions of interest (ROIs) are in use, mainly for research purposes, to calculate activity uptake in the striatum relative to the background. The measured uptake ratios highly depend on the spatial resolution of the SPECT images, which can be more than 10 mm, measured as full width at half maximum of a point source. The limited spatial resolution together with the finite voxel size cause the so-called partial-volume effect, which can be described as spill-in and spill-out of counts between different regions (*12*). Small regions in particular are sensitive to the partial-volume effect, and since the striatum consists of relatively small structures (the caudate nucleus and putamen), the measured uptake ratios are severely affected by this effect. Spatial resolution in SPECT is primarily dependent on collimator characteristics, reconstruction methods, and image filtering but is also dependent on the rotation radius of the γ-camera detectors. It is therefore important to position the detectors as close to the patient as possible so as not to unnecessarily degrade spatial resolution. Dedicated brain

SPECT systems may have a fixed rotation radius such as the Neurocam (GE Healthcare) or may be based on multiple-pinhole technology (13), but most brain SPECT studies are performed using multipurpose γ-cameras with parallel-hole collimators and an adjustable rotation radius. The rotation radius for brain SPECT is typically set to a constant value to keep resolution constant, especially if the images are evaluated with semiquantitative methods for research purposes. At the Nuclear Medicine Department at the University Hospital of Umeå, the preferred rotation radius for brain SPECT is 15 cm. Because of variations in patient compliance (e.g., claustrophobia) or body constitution (e.g., a short or stiff neck), or if the patient has a cervical ailment, a larger rotation radius may, however, be required.

The aim of this study was to evaluate the effect of a varying rotation radius for dopamine brain SPECT and, if needed, to develop correction factors, as a function of rotation radius, that will recalculate measured uptake ratios so that they become equivalent to a study with a 15-cm rotation radius. Monte Carlo simulations were used, and are convenient for this purpose, since the rotation radius easily can be varied and the activity distribution in a simulated clinically realistic phantom can be set to be constant over time. The aim was not to completely correct partial-volume effect, which would be difficult in a clinical setting. The intention was to study uptake corresponding to ^{123}I-FP-CIT and ^{123}I-IBZM separately, since these images differ in contrast. The uptake ratios are, on average, a factor of 2.4 higher for ^{123}I-FP-CIT than for ^{123}I-IBZM for healthy subjects at Norrland's University Hospital. At present, we use 2 different methods for deriving uptake ratios, one based on 2-dimensional (2D) ROIs and one on 3-dimensional (3D) volumes of interest (VOIs), and the aim was to evaluate both methods.

MATERIALS AND METHODS

Monte Carlo Simulations

The ^{123}I-FP-CIT and ^{123}I-IBZM brain SPECT images were simulated using the Monte Carlo program SIMIND (14), and the option to include photon interactions and penetration effects in a parallel-hole collimator was used (15). The simulations were designed to match methods and equipment used in clinical routine at the Nuclear Medicine Department at the University Hospital of Umeå. All simulations were performed with specifications according to the γ-camera part of an Infinia Hawkeye SPECT/CT system (GE Healthcare) with 0.95-cm-thick NaI crystals, equipped with low-energy general-purpose collimators. The spatial resolution using this collimator is 9.0 mm at a distance of 10.0 cm free in air, according to specifications. The Infinia SPECT system is a dual-head multipurpose γ-camera, and the SPECT simulations were performed for 120 equally spaced projection angles in a 360° stepwise rotation. The following radii of rotation were simulated: 14, 15, 17, 19, 21, and 23 cm. The full energy spectrum of ^{123}I was simulated, and a main energy window of 20% centered at 159 keV was used. Two scatter windows, each with a width of 15.9 keV, were placed edge to edge at each side of the main window and were used for triple-energy-window scatter correction (16). The energy resolution of the SPECT system has been measured to 8.9% full width at half maximum for 140-keV photons, and this

was used also for the simulations. The images were simulated in 128×128 pixel matrices with a pixel size of 2.95×2.95 mm. The total number of photons per projection image was set to 4.5×10^8 for each simulation.

A voxel-based brain phantom (17,18) was used to simulate the brain SPECT images. As in previous studies (19–21), the densities of the different brain structures were set to 1.04 g/cm³ for brain tissue, 1.30 g/cm³ for the skull (average bone density according to the International Commission on Radiological Protection (22)), and 0.60 g/cm³ for the low-density regions (mouth cavity and sinuses) (23). For simulations of the high uptake ratio, corresponding to uptake of ^{123}I-FP-CIT for a healthy subject, the relative activity concentrations were set to 16 in the striatal structures and 3 in the rest of the brain. These values reflect an uptake that, when measured with semiquantitative analysis on the reconstructed images, is within the SD of what is considered to be representative for a healthy subject. For the ^{123}I-IBZM simulations, the relative activity concentrations in different brain structures can be seen in Table 1. Because data for actual ^{123}I-IBZM uptake in the human brain are scarce, the simulated phantom is a combination of data from in-house observations and from the literature and has been described in detail in a previous publication (21). The data are intended to reflect a healthy subject, and the measured uptake ratio is also in this case within the SD of healthy individuals imaged with ^{123}I-IBZM. This relatively low uptake ratio corresponds, however, fairly well also to a ^{123}I-FP-CIT study for a patient with a parkinsonian syndrome. For both phantom definitions, activity was also defined outside the brain to simulate blood background and uptake of free iodine in the parotid glands, but no out-of-field activity was simulated.

Reconstruction

The simulated images had much lower relative noise levels than are seen in clinical examinations. No extra noise was added to the images because a low noise level was considered to be advantageous for the ROI setting and the semiquantitative measurements in this study. All images were reconstructed on the clinical workstation Xeleris (GE Healthcare) using a clinical protocol based on ordered-subsets expectation maximization (2 iterations, 10 subsets). Attenuation correction was performed using an inhomogeneous attenuation map calculated from the densities of

TABLE 1
Activity Concentrations in ^{123}I-IBZM Phantom

Structure	Activity concentration
Gray matter	62
White matter	54
Cerebellum	43
Striatum	170
Hippocampus	128
Globus pallidus	108
Thalamus	68
Amygdala	68
Pituitary gland	70
Soft tissues outside brain	13
Ventricles	0

An arbitrary unit can be assumed since only relative ratios are of importance for analyses in this study.

the phantom, and the same attenuation map was used for all reconstructions. Scatter was corrected using a triple-energy window. Butterworth postfiltering with a cutoff frequency of 0.45 cm^{-1} and a power factor of 8 was also performed.

Evaluation

Images were analyzed by an experienced nuclear medicine specialist using 2 different methods, a semiautomatic ROI method, using in-house template ROIs (24), and commercial automatic VOI-based software, EXINI dat (EXINI Diagnostics AB). Both methods were developed for reconstructed SPECT image data, and no anatomic information is required. All images were analyzed 3 times with both methods, with at least 3 d between each evaluation, and the average values of the results were used. The images corresponding to the high uptake ratio and lower uptake ratio were studied separately.

The simulated phantom image data were reoriented during reconstruction to get transversal slices in the occipitomeatal plane, with the striatal and the occipital region in the same transversal slices. When the ROI-based analysis was used, a representative transversal image, usually the one with the highest mean counts in the striatum, was chosen for ROI definition. Two template ROIs representing the putamen and caudate nucleus were then placed over the striatum in each hemisphere. An ROI representing the whole striatum in each hemisphere was calculated as a superposition of the putaminal and caudate ROIs, and an ROI in the occipital lobe was used as the reference region. The ROIs were positioned in the respective region to cover the highest mean uptake in the striatum and the most representative mean uptake in the occipital lobe. The ROIs were constant in size and geometric shape but could be freely rotated and moved to fit each individual image. The ROIs were then automatically copied to the 3 adjacent transversal images containing the highest mean counts, considered to be the most representative images for uptake in the striatum. The average value for all 4 slices was used for the analysis, which means that the results were calculated from a 12-mm-thick image slab through the striatum. The semiquantitative analysis was performed by dividing the average number of counts in the caudate, putaminal, or striatal ROI by the average number of counts in the occipital ROI. Detailed information about the ROI method can be found in a previous paper (24).

The novel EXINI dat software is a possible future alternative to the ROI method. The software is intended for DAT images and adapts 3D VOIs to the brain and the striatal regions, which are divided into the putamen and the caudate nucleus. Two reference regions can be chosen from either the occipital cortex or the "whole brain," where the whole brain is intended to represent cortical uptake. In this study, we chose the occipital region as the reference region to get similar reference regions for both methods. The VOIs are adapted to the data automatically, but manual adjustments are possible. The VOIs are constant in size and shape, and the semiquantitative analysis is calculated as the specific uptake, (S − B)/B, where S is the average value in the caudate, putaminal, or striatal VOI and B is the average value in the background VOI. The specific uptake is also multiplied by a constant factor of 2.5, which is included in the software as an approximate correction for the average partial-volume effect.

The semiquantitative ratios were then used to calculate correction factors for each rotation radius. A rotation radius of 15 cm was the defined reference in our method, and we aimed to recalculate measured uptake ratios with a deviating rotation radius. Correction factors were calculated by dividing the uptake ratio at 15 cm by the ratios from the other radii. The results were plotted as a function of the radius minus 15 cm. Because resolution is linearly dependent on distance from the collimator (25), at least after the first few centimeters, a linear function was fitted to the correction factors.

RESULTS

The ROIs used by the ROI method, applied to one of the simulated phantom images (^{123}I-FP-CIT, 15-cm radius of rotation), are presented in Figure 1. As mentioned, the ROIs were applied on a 12-mm-thick slab through the striatal and occipital region.

The calculated correction factors for different rotation radii for the ROI method are presented in Figure 2A for the higher uptake ratio. The corresponding fitted linear equations, with R^2 values, are as follows:

$$C_{Ca} = 0.0139(R-15)+1.001 \; (R^2 = 0.933),$$

$$C_{Pu} = 0.0114(R-15)+1.009 \; (R^2 = 0.973),$$

$$C_{St} = 0.0120(R-15)+1.009 \; (R^2 = 0.930).$$

C is the correction factor to be multiplied by the measured uptake ratio, and the subscripts Ca, Pu, and St denote caudate nucleus, putamen, and striatum, respectively. R is the rotation radius measured in centimeters. From the slopes of the linear equations, it can be seen that there is an average change in uptake ratio of 1.2%/cm of increasing rotation radius.

For the lower uptake ratio, corresponding to the ^{123}I-IBZM uptake according to Table 1, the results for the ROI method are presented in Figure 2B and the fitted linear equations can be written as follows:

$$C_{Ca} = 0.0099(R-15)+1.002 \; (R^2 = 0.985),$$

$$C_{Pu} = 0.0083(R-15)+0.998 \; (R^2 = 0.990),$$

$$C_{St} = 0.0090(R-15)+1.000 \; (R^2 = 0.995).$$

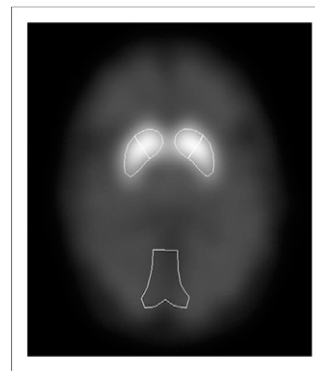In this case, there is an average change of about 0.9%/cm of increasing rotation radius.

FIGURE 1. ROIs used by ROI method, applied on high-uptake-ratio image (rotation radius, 15 cm). ROIs are applied on 12-mm-thick slab through striatal and occipital region.

FIGURE 2. Correction factors for high (A) and low (B) uptake ratios measured with in-house ROI method. R is rotation radius measured in centimeters.
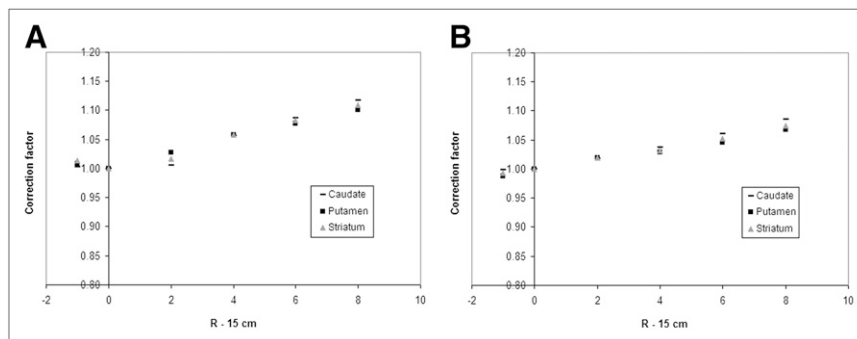
The EXINI dat VOIs applied to one of the simulated phantom images (^{123}I-FP-CIT, 17-cm radius of rotation) are presented in Figure 3. For this method, the results for the higher uptake ratio are presented in Figure 4A and the linear equations fitted to the data are as follows:

$$C_{Ca} = 0.0196(R - 15) + 0.993 \ (R^2 = 0.986),$$

$$C_{Pu} = 0.0215(R - 15) + 0.990 \ (R^2 = 0.965),$$

$$C_{St} = 0.0205(R - 15) + 0.991 \ (R^2 = 0.982).$$

According to the equations, the average change in uptake ratio per centimeter of increasing rotation radius is in this case about 2.1%, which clearly makes this method more dependent on the rotation radius than is the ROI-based technique. The corresponding results for the lower uptake ratio for the EXINI dat method can be seen in Figure 4B with the following fitted linear equations:

$$C_{Ca} = 0.0170(R - 15) + 0.994 \ (R^2 = 0.984),$$

$$C_{Pu} = 0.0180(R - 15) + 1.004 \ (R^2 = 0.958),$$

$$C_{St} = 0.0174(R - 15) + 0.999 \ (R^2 = 0.996).$$

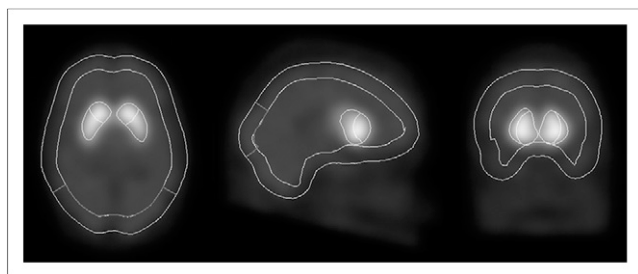In this case, the average change in uptake ratio per centimeter is on the order of 1.7%.

FIGURE 3. VOIs used by EXINI dat, demonstrated on high-uptake-ratio image (rotation radius, 17 cm). Caudate and putaminal VOIs are presented together with whole-brain background VOI, including occipital VOI.

DISCUSSION

In this study, the rotation radius dependence of uptake ratios for dopamine brain SPECT was investigated. The spatial resolution of the SPECT images decreases with increasing rotation radius, leading to more spill-out from the striatal ROIs and VOIs. The higher degree of spill-in does not compensate for this effect, because of the lower activity concentration in structures surrounding the striatum. We had no intention of doing a complete correction for the partial-volume effect in order to calculate true uptake ratios, since these methods usually rely on an anatomic definition of the striatal contours, which would be difficult to apply in SPECT studies. If the dependence on rotation radius turned out to be significant, we were instead interested in correcting the measured uptake ratios to a reference rotation radius, which is 15 cm for brain SPECT in the clinical protocol at the University Hospital of Umeå. Monte Carlo simulations were used to produce images for a digital brain phantom for 2 different activity distributions, each with 8 different rotation radii. Correction factors were then derived as a function of the deviation of the rotation radius from 15 cm. A linear dependence was assumed and was also found to correspond fairly well to the data for this limited range of rotation radii, 14–23 cm. For simplicity, only a single phantom image per point in the diagrams was used, and these images had low noise levels to facilitate ROI positioning and to decrease the noise dependence on the results. Because no noise-dependent model-based corrections were used in this project, such as compensation for detector response, the use of low-noise images should not introduce any bias. All images were analyzed 3 times, and the average uptake ratios were calculated.

Two semiquantitative techniques for measuring uptake ratios were used, an in-house ROI method that measures uptake ratios from reoriented 12-mm-thick image planes, and the software EXINI dat, which adapts 3D VOIs to the image volumes. The rotation radius dependence is described by the slope of the linear equations, and it is clear that the EXINI dat method is more affected by differences in rotation radius than is the ROI method. EXINI dat and the ROI method use somewhat different techniques to calculate the uptake ratios, but this difference should have no effect on the slopes. Instead, the steeper slopes result from the fact that 3D
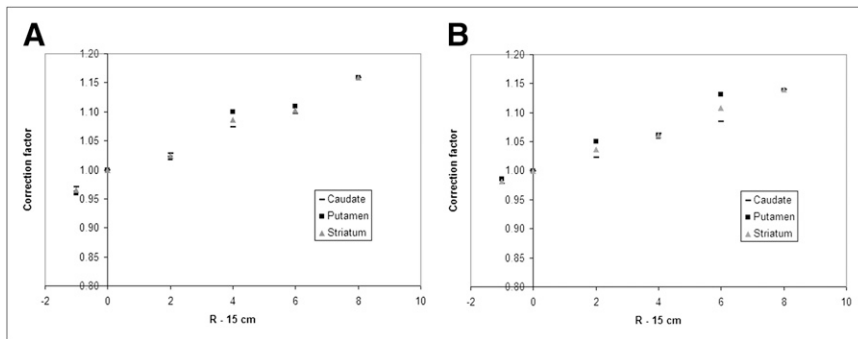
FIGURE 4. Correction factors for high (A) and low (B) uptake ratios measured with EXINI dat software. R is rotation radius measured in centimeters.

volumes are relatively more affected by partial-volume effect than are 2D slices. It should, however, be noted that the ROIs also are affected by some of the volume effects since the ROIs are applied on a relatively thick slab, 12 mm, although that does not cover the whole striatal volume. From the results, one can also conclude that the slopes for the higher uptake ratio are steeper than those for the lower uptake ratio, as was expected. The images with lower uptake ratio are more affected by spill-in from the structures surrounding the striatum, compared with the higher uptake ratios, and are therefore less affected by changes in rotation radius.

According to the results, the uptake ratio decreased about 0.8%–2.2%/cm of increased rotation radius. The effect is therefore comparable to other uncertainties, such as ROI/VOI positioning, patient movement, and noise, for a moderate deviation of a few centimeters from the reference radius. We consider this effect significant, and we therefore intend to apply these corrections, when needed, to improve reference limits and follow-up. For the healthy controls included in the research project NYPUM (*11*), the derived equations can readily be used for ^{123}I-FP-CIT and ^{123}I-IBZM, but when patients are considered, the choice of corrections becomes more complex. As mentioned, the simulated lower uptake ratio can correspond also to a ^{123}I-FP-CIT study for a patient with a parkinsonian syndrome. However, patients are not a homogeneous group and the uptake ratios for patients can vary from very low values to close to normal. Fortunately, the differences between the correction factors for the higher and lower uptake ratio were quite small. The slopes of the correction equations for the lower uptake ratio were on average 73% of those of the higher uptake ratio for the ROI method and 85% for EXINI dat. Thus, no major errors are introduced in that interval of uptake ratios if the correction factors for the low uptake ratio are used for all patients. For ^{123}I-FP-CIT studies of patients in advanced stages of idiopathic Parkinson disease and for ^{123}I-IBZM studies of patients with atypical parkinsonism, even lower uptake ratios can be expected, which would benefit from lower correction factors. Because of the small difference between the high and low uptake ratio in this study, we expect, however, no major errors from using the low uptake ratio corrections also for these groups of patients. An alternative could be to use no correction at all for the lowest

uptake ratios, but we believe that it is better to be consistent in those cases to make sure that the same correction equations are used for baseline and follow-up examinations.

Figures 2 and 4, together with the R^2 values from the corresponding equations, showed some uncertainties when the data were fit to a straight line, for both methods. The ROI method showed the best results for the low uptake ratio, whereas EXINI dat had equivalent R^2 values for both uptake ratios. Because of these uncertainties, and for the sake of simplicity, it should be possible to use the correction equations for the whole striatum also for the caudate and putaminal ROIs and VOIs.

The images in this study were corrected for both attenuation and scatter. These corrections are advantageous for the quantitative accuracy of the SPECT image data but are not required for implementation of the methodology described in this study. SPECT images that are not corrected for scatter can be expected to be somewhat less affected by changes in rotation radius because of the lower contrast when scatter correction is omitted.

CONCLUSION

For a moderate deviation of a few centimeters from the reference rotation radius, the effect on the uptake ratios is significant, especially for the VOI method. The decrease in uptake ratio with increasing rotation radius can be corrected using linear equations, but the equations derived in this study are valid only for the described equipment and methods of analysis.

ACKNOWLEDGMENTS

REFERENCES

1. Hesse S, Oehlwein C, Barthel H, et al. Possible impact of dopamine SPECT on decision-making for drug treatment in Parkinsonian syndrome. *J Neural Transm.* 2006;113:1177–1190.
2. Benamer TS, Patterson J, Grosset DG, et al. Accurate differentiation of parkinsonism and essential tremor using visual assessment of (^{123}I)-FP-CIT SPECT imaging: the (^{123}I)-FP-CIT study group. *Mov Disord.* 2000;15: 503–510.

3. Marshall V, Grosset D. Role of dopamine transporter imaging in routine clinical practice. *Mov Disord.* 2003;18:1415–1423.

4. Vlaar AM, van Kroonenburgh MJ, Kessels AG, Weber WE. Meta-analysis of the literature on diagnostic accuracy of SPECT in parkinsonian syndromes. *BMC Neurol.* 2007;7:27.

5. Lorberboym M, Treves TA, Melamed E, Lampl Y, Hellmann M, Djaldetti R. (123I)-FP/CIT SPECT imaging for distinguishing drug-induced parkinsonism from Parkinson's disease. *Mov Disord.* 2006;21:510–514.

6. Kung HF, Pan S, Kung MP, et al. In vitro and in vivo evaluation of (1-123) IBZM: a potential CNS D-2 dopamine receptor imaging agent. *J Nucl Med.* 1989;30:88–92.

7. Videbaek C, Toska K, Scheideler MA, Paulson OB, Knudsen GM. SPECT tracer (123I)IBZM has similar affinity to dopamine D2 and D3 receptors. *Synapse.* 2000;38:338–342.

8. Kim YJ, Ichise M, Ballinger JR, et al. Combination of dopamine transporter and D2 receptor SPECT in the diagnostic evaluation of PD, MSA, and PSP. *Mov Disord.* 2002;17:303–312.

9. Plotkin M, Amthauer H, Klaffke S, et al. Combined 123I-FP-CIT and 123I-IBZM SPECT for the diagnosis of parkinsonian syndromes: study on 72 patients. *J Neural Transm.* 2005;112:677–692.

10. van Royen E, Verhoeff NF, Speelman JD, Wolters EC, Kuiper MA, Janssen AG. Multiple system atrophy and progressive supranuclear palsy: diminished striatal D2 dopamine receptor activity demonstrated by 123I-IBZM single photon emission computed tomography. *Arch Neurol.* 1993;50:513–516.

11. Linder J, Stenlund H, Forsgren L. Incidence of Parkinson's disease and parkinsonism in northern Sweden: a population-based study. *Mov Disord.* 2010;25:341–348.

12. Ritt P, Vija H, Hornegger J, Kuwert T. Absolute quantification in SPECT. *Eur J Nucl Med Mol Imaging.* 2011;38(suppl 1):S69–S77.

13. Goorden MC, Rentmeester MC, Beekman FJ. Theoretical analysis of full-ring multi-pinhole brain SPECT. *Phys Med Biol.* 2009;54:6593–6610.

14. Ljungberg M, Strand SE. A Monte Carlo program for the simulation of scintillation camera characteristics. *Comput Methods Programs Biomed.* 1989;29:257–272.

15. Ljungberg M, Larsson A, Johansson L. A new collimator simulation in SIMIND based on the delta-scattering technique. *IEEE Trans Nucl Sci.* 2005;52:1370–1375.

16. Ogawa K, Harata Y, Ichihara T, Kubo A, Hashimoto S. A practical method for position-dependent Compton-scatter correction in single photon emission CT. *IEEE Trans Med Imaging.* 1991;10:408–412.

17. Zubal IG, Harrell CR, Esser PD. Monte Carlo determination of emerging energy spectra for diagnostically realistic radiopharmaceutical distributions. *Nucl Instrum Methods Phys Res.* 1990;A299:544–547.

18. Zubal IG, Harrell CR. Voxel based Monte Carlo calculations of nuclear medicine images and applied variance reduction techniques. *Image Vis Comput.* 1992;10:342–348.

19. Larsson A, Ljungberg M, Jakobson Mo S, Riklund K, Johansson L. Correction for scatter and septal penetration using convolution subtraction methods and model-based compensation in 123I brain SPECT imaging: a Monte Carlo study. *Phys Med Biol.* 2006;51:5753–5767.

20. Larsson A, Jakobson Mo S, Sundström T, Riklund K. Gaussian prefiltering of 123I DAT SPECT images when using depth-independent resolution recovery. *Phys Med Biol.* 2007;52:N393–N399.

21. Larsson A, Jakobson Mo S, Ljungberg M, Riklund K. Dopamine D2 receptor SPECT with 123I-IBZM: evaluation of collimator and post-filtering when using model-based compensation: a Monte Carlo study. *Phys Med Biol.* 2010;55:1971–1988.

22. *ICRP Publication 89: Basic Anatomical and Physiological Data for Use in Radiological Protection: Reference Values.* Amsterdam, The Netherlands: Elsevier; 2003.

23. Ärlig Å, Gustafsson A, Jacobsson L, Ljungberg M, Wikkelsö C. Attenuation correction in quantitative SPECT of cerebral blood flow: a Monte Carlo study. *Phys Med Biol.* 2000;45:3847–3859.

24. Mo SJ, Linder J, Forsgren L, Larsson A, Johansson L, Riklund K. Pre- and postsynaptic dopamine SPECT in the early phase of idiopathic parkinsonism: a population-based study. *Eur J Nucl Med Mol Imaging.* 2010;37:2154–2164.

25. Anger HO. Radioisotope cameras. In: Hine GJ, ed. *Instrumentation in Nuclear Medicine 1.* New York, NY: Academic Press; 1967:485–552.